ce/papers Proceedings in civil engineering

Ernst & Sohn A Wiley Brand

Check for updates

ORIGINAL ARTICLE

eurosteel AMSTERDAM 2023

Ernst & Sohn A Wiley Brand

Monotonic and cyclic behaviour of 6082-T6 aluminium alloy

Evangelia Georgantzia[1] | Mohammad M Kashani [1]

Correspondence

Dr. Evangelia Georgantzia
School of Engineering
Infrastructure Research Group
Bolderwood Innovation Campus
Room 3019, Building 178
Burgess Road
SO16 7QF, Southampton
United Kingdom
Email: E.Georgantzia@soton.ac.uk

[1] University of Southampton, Southampton, United Kingdom

Abstract

Over the last few decades, the application of 6000 series aluminium alloys as structural material has been increased owing to their favourable properties. Many research studies on the monotonic behaviour have been reported, whilst the studies investigating the cyclic behaviour are quite limited. To address this gap, an experimental campaign is currently underway to investigate the nonlinear stress-strain behaviour of 6000 series aluminium alloys. This paper presents and discusses preliminary experimental results on the stress-strain behaviour of 6082-T6 aluminium alloy under monotonic and cyclic loading. Particularly, tensile, and variable amplitude cyclic coupon tests are executed to determine the mechanical properties of 6082-T6 aluminium alloy. The obtained failure modes as well as the monotonic and hysteretic curves are presented and discussed. It was found that at increased strain demands the examined aluminium alloy exhibited hardening behaviour without material degradation demonstrating its potential for structural application in earthquake prone areas. The experimental curves are also utilised to assess the accuracy of existing theoretical models for monotonic and cyclic envelope curves. Finally, the need for a constitutive model capable of predicting the hysteretic behaviour of 6,000 series aluminium alloys is highlighted.

Keywords

Aluminium alloys, Cyclic testing, Hysteretic curve, Envelope curve

1 Introduction

Over the last 20 years, 6000 series aluminium alloys have gained great interest in the construction sector owing to their favourable properties. Particularly, 6000 series aluminium alloys are characterised by low density and high strength-to-weight ratio which make them a suitable choice for high-rise buildings and long-span structures (see Figures 1 and 2 [1,2]).

Figure 1 Casablanca Finance City Tower, Casablanca, Morocco (2019).

Figure 2 Ferrari World, Abu Dhabi, UAE (2010).

Moreover, the adequate corrosion resistance coupled with great durability encourage the usage of this material in structural applications where low maintenance demand is a primary concern. Within the framework of sustainability and climate-change mitigation commitments, the high potential of recycling and reuse of aluminium alloys are important aspects that should be considered during the material choice. It is noteworthy that the low self-weight and considerable ductility could extend the application of 6000 series aluminium alloys in structures in earthquake prone regions. Under seismic loading conditions, the structural

https://doi.org/10.1002/cepa.2315 wileyonlinelibrary.com/journal/cepa

members and particularly those acting as dissipative elements, exhibit small numbers of very large displacement cycles. The structural performance of these members under this type of loading is governed mainly by their geometrical properties as well as the hysteretic behaviour of the constituent material [3,4]. To date, numerous studies on the structural behaviour of 6000 series aluminium alloys under monotonic loading have been conducted and different constitutive models have been established [5-10]. Nonetheless, the reported research on the cyclic behaviour is quite limited [11]. Particularly, Hopperstad et al. [12] performed uniaxial cycling tests on 6060-T4 and 6060-T5 coupon specimens under constant and varying strain amplitudes up to 1.2%. Upon tests, the cyclic plasticity model of Chaboche [13] was modified to consider the Bauschinger effect exhibited by 6060-T4 alloy. In a following study [14], the same authors conducted biaxial proportional and non-proportional cycling tests and extended the previous constitutive model to capture the observed influence of the strain range and the strain path shape on the material hardening. The aforementioned tests were executed under low strain amplitudes (<2%) and thus could not clarify the presence of material hardening behaviour. To this end, Dusicka & Tinker [15] investigated experimentally the hysteretic response of 6061-T6/511coupon specimens subjected to constant strain amplitudes beyond 2% and up to 4%. The observed slight increase of the cyclic softening behaviour indicated its potential for seismic retrofit applications. Recently, Guo et al. [16] performed cyclic tests on 6082-T6 and 7020-T6 aluminium alloys applying strain amplitudes up to 4%. A new constitutive model for the hysteretic behaviour of aluminium alloys was also proposed using. the reduction factor method.

Aiming to supplement the existing literature, an experimental campaign is currently underway to investigate the nonlinear stress-strain behaviour of 6000 series aluminium alloys. This paper presents and discusses preliminary experimental results on the stress-strain behaviour of 6082-T6 aluminium alloy under monotonic and cyclic loading up to 6.5% amplitude. Upon a brief introduction in Section 1, Section 2 includes a detailed presentation of the coupon specimens along with the set-ups employed in the tests. Section 3 analyses the results obtained from the monotonic and cyclic tests. Finally, conclusions based on this study are summarised in Section 4.

2 Experimental programme

2.1 Geometry of test specimens

In total 6 material tests were conducted in the Testing and Structures Research Laboratory of the Department of Civil, Maritime and Environmental Engineering at University of Southampton to examine the monotonic and hysteretic stress-strain response of 6082-T6 aluminium alloy. The monotonic tensile tests were performed on flat coupons extracted from tubular specimens with 3.3 mm thickness and machined in line with the geometric requirements described in EN ISO 6892-1 [17]. The geometry of the coupons is shown in Figure 3(a). The coupons subjected to cyclic tests were also extracted from the same tubular specimens and were designed according to the ASTM E606-04 standard [18] (Figure 3(b)). As can be seen the adopted gauge length for the coupons subjected to cyclic loading is smaller compared to that of the coupons subjected to monotonic loading to prevent premature failure due to buckling at the compression stage.

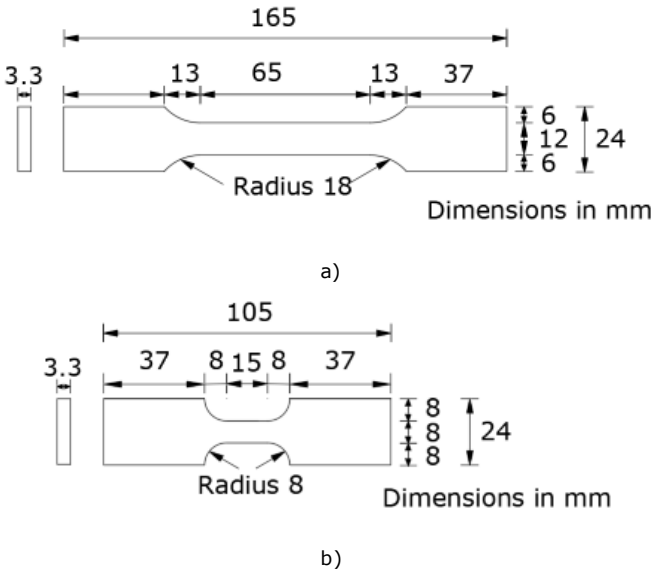

Figure 3 Geometry of specimens for a) monotonic tensile loading and b) cyclic loading.

2.2 Test setup and loading protocol

A 250 kN Instron machine was used to apply monotonic tensile loading under displacement control and at a displacement rate of 0.2 mm/min. An extensometer with gauge length of 50mm was mounted onto the central necked part of each coupon to record the longitudinal strains during testing (Figure 4).

Figure 4 Monotonic tensile test setup.

The same testing machine and setup were employed to perform the cyclic tests. However, an extensometer with gauge length of 12.5 mm was used due to smaller gauge length of the coupon specimen. A two-cycle reversed symmetrical strain history up to 6.5% amplitude was applied as shown in Figure 5. This loading protocol was similar to Kashani et al. [19] and enabled to study the nonlinear cyclic behaviour at high strain demand levels.

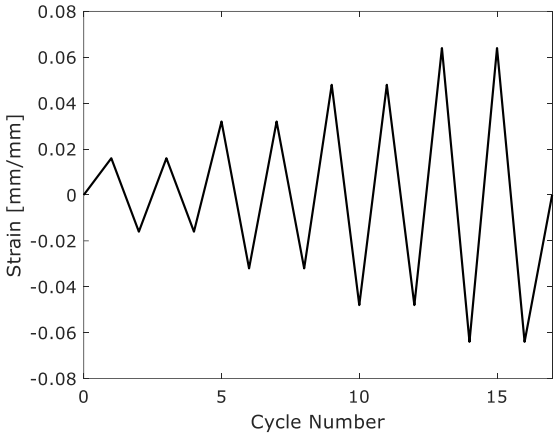

Figure 5 Loading protocol for cyclic tests.

3 Experimental results and discussion

3.1 Monotonic tensile tests

All tested coupon failed brittle with apparent necking close to the fracture section. The measured material properties, including the initial modulus of elasticity E, the 0.05 % proof stress $\sigma_{0.05}$, the 0.1 % proof stress $\sigma_{0.1}$, the 0.2 % proof stress $\sigma_{0.2}$, the 1 % proof stress $\sigma_{1.0}$, the ultimate tensile stress σ_u, the strain corresponding to ultimate tensile stress ε_u, the strain at fracture ε_f, and the strain hardening exponent n [20,21] are summarised in Tables 1 and 2. The strain hardening ratio $\sigma_u/\sigma_{0.2}$ for each examined coupon is also listed in Table 2, reaching up to 112%. The adopted notation for the coupon specimens indicates the type of the aluminium alloy, the type and the number of the test. For example, the label "6082-T6-M1" represents a coupon specimen made form 6082-T6 aluminium alloy which tested 1st under monotonic tensile loading. Figure 6 shows the experimental stress-strain curves, whilst Figures 7(a) and 7(b) depict the 6082-T6-M1 coupon after tensile fracture and all coupons after monotonic tensile testing, respectively.

Table 1 Material properties obtained from monotonic tensile tests.

Specimen	E (MPa)	$\sigma_{0.05}$ (MPa)	$\sigma_{0.1}$ (MPa)	$\sigma_{0.2}$ (MPa)	$\sigma_{1.0}$ (MPa)
6082-T6-M1	66638	252	258	264	274
6082-T6-M2	60182	257	260	267	275
6082-T6-M3	73081	256	261	269	280

Table 2 Material properties obtained from monotonic tensile tests.

Specimen	σ_u (MPa)	ε_u (%)	ε_f (%)	n	$\sigma_u/\sigma_{0.2}$ (%)
6082-T6-M1	296	9.18	13.68	31.84	112
6082-T6-M2	299	7.93	16.13	26.95	112
6082-T6-M3	302	8.43	13.50	22.40	112

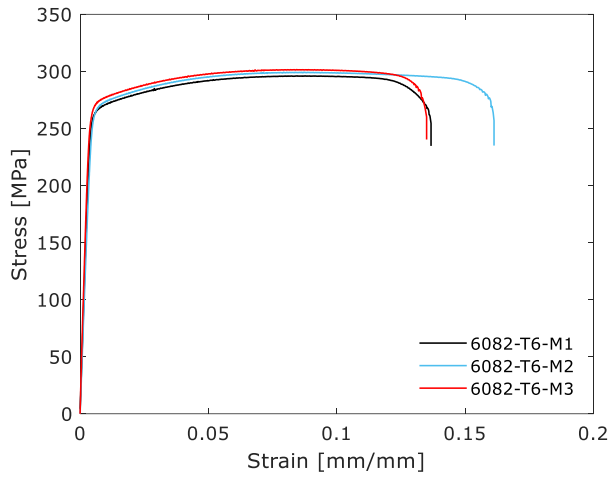

Figure 6 Material properties obtained from monotonic tensile tests.

a) b)

Figure 7 a) 6082-T6-M1 coupon after tensile fracture and b) all coupons after monotonic tensile testing.

As can be seen from Figure 6, the engineering stress–strain response of 6082-T6 aluminum alloy is characterized by a continuous rounded curve with an absence of a sharply defined yield point. The two-stage model proposed by Yun et al. [10] was used herein to reproduce the experimentally obtained stress-strain curves. Particularly, this model uses the following Equations (1)-(4) to produce the stress–strain curves of 5,000, 6,000 and 7,000 series aluminium alloys over the full range of tensile strains up to the ultimate tensile strain.

$$\varepsilon = \begin{cases} \dfrac{\sigma}{E} + 0.002\left(\dfrac{\sigma}{\sigma_{0.2}}\right)^n, & \text{for } 0<\sigma \le \sigma_{0.2} \\ \dfrac{\sigma-\sigma_{0.2}}{E_{0.2}} + \left(\varepsilon_u - \varepsilon_{0.2} - \dfrac{\sigma_u-\sigma_{0.2}}{E_{0.2}}\right)\left(\dfrac{\sigma-\sigma_{0.2}}{\sigma_u-\sigma_{0.2}}\right)^m + \varepsilon_{0.2}, & \text{for } \sigma_{0.2}<\sigma \le \sigma_u \end{cases} \quad (1)$$

where ε is the strain, σ is the stress, $\varepsilon_{0.2}$ is the yield strain and $E_{0.2}$ is the tangent modulus at the yield strength given by Equation (2). The parameters n and m are given from the Equations (3) and (4), respectively.

$$E_{0.2} = \frac{E}{1 + 0.002n\dfrac{E}{\sigma_{0.2}}} \quad (2)$$

$$n = \frac{\ln(4)}{\ln\left(\frac{\sigma_{0.2}}{\sigma_{0.05}}\right)} \quad (3)$$

$$m = \frac{\ln\left(0.008 + \frac{\sigma_{1.0} - \sigma_{0.2}}{E} - \frac{\sigma_{1.0} - \sigma_{0.2}}{E}\right) - \ln\left(\varepsilon_u - \varepsilon_{0.2} - \frac{\sigma_u - \sigma_{0.2}}{E_{0.2}}\right)}{\ln(\sigma_{1.0} - \sigma_{0.2}) - \ln(\sigma_u - \sigma_{0.2})} \quad (4)$$

The accuracy of the model [10] is assessed by comparing a representative predicted curve with the corresponding experimental stress-strain curve (Figure 8). Both curves are in good agreement showing that this model [10] yields accurate representation of the experimental stress–strain behaviour. The same was also concluded comparing the predicted with the experimental curves for the other two tested coupons. Therefore, the model suggested by Yun et. Al [10] is suitable for describing the monotonic behaviour of the 6082-T6 aluminium alloy.

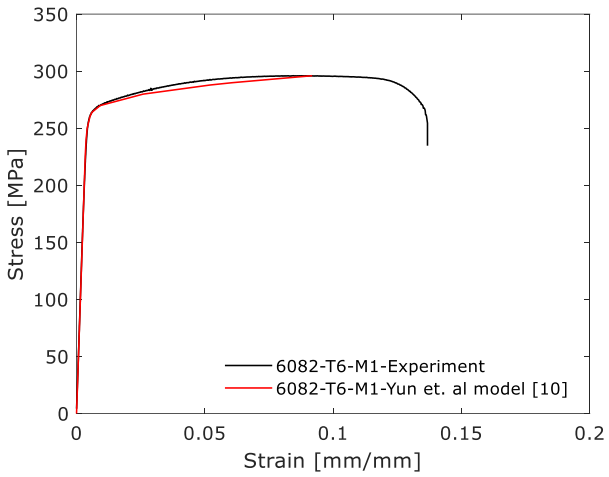

Figure 8 Experimental and theoretical monotonic stress-strain curves.

3.2 Cyclic tests

The stress-strain responses obtained from the cyclic coupon tests are shown in Figure 9. It is noted that tension is positive, and compression is negative in these graphs. As can be observed, the obtained hysteretic loops are relatively plump denoting satisfactory hysteretic behaviour and adequate energy dissipation capacity of the examined aluminium alloy. As was expected, the small gauge length of the tested coupons limited the occurrence of buckling and thus there was no degradation in the compressive strength before the end of the tests. Moreover, the second cycle at each strain demand level did not result in a significant cyclic degradation and the response was almost identical to the first cycle. When the strain demand increased beyond the yield strain, a kinematic combined with slight isotropic hardening behaviour was observed and continued by the end of the test. In order to assess the influence of the cycling loading on the material behaviour, the monotonic tension envelopes were also plotted in Figure 9. It can be seen that both the tension envelope curves under monotonic and cyclic loading follow the same trend, although the latter ones exhibit a slight hardening behaviour.

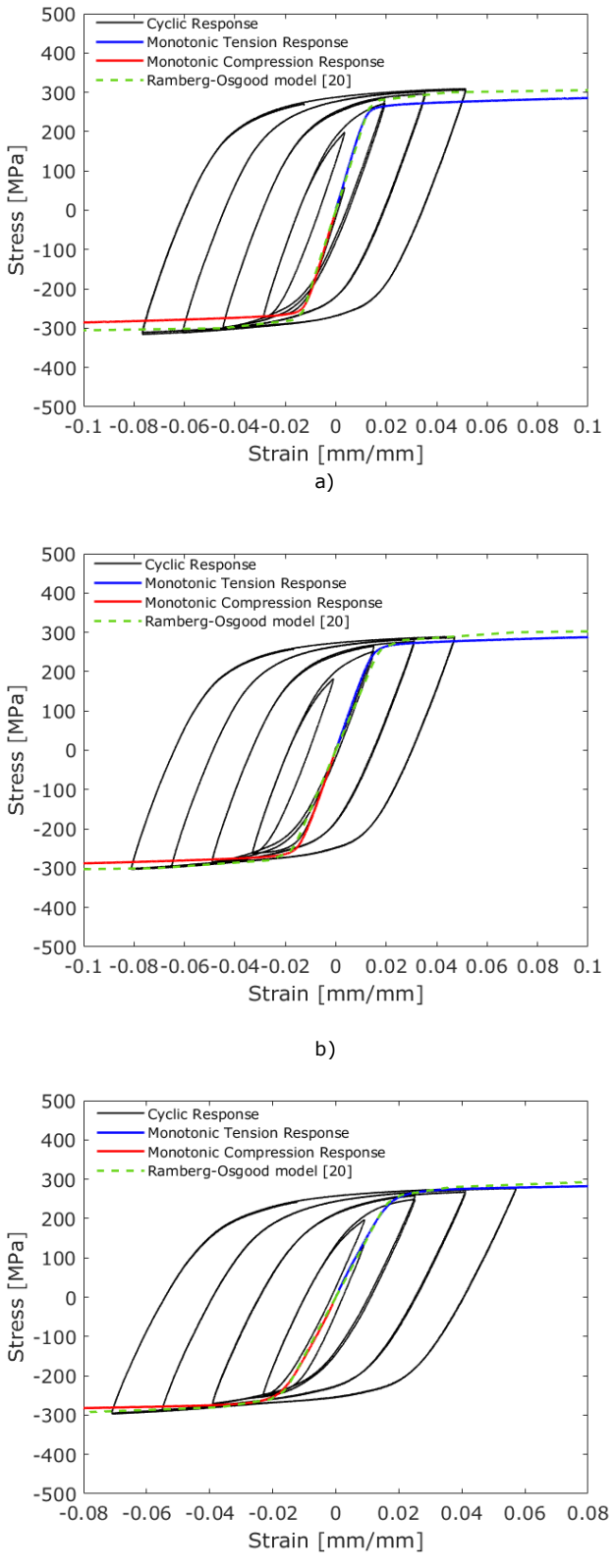

Figure 9 Stress-strain responses obtained from cyclic coupon tests a) 6082-T6-C1, b)6082-T6-C2 and c) 6082-T6-C3.

The cyclic envelope curves were modelled using a power law relationship that consisted of an elastic component and the Ramberg–Osgood model [20] for the plastic strain component as described in Equation (5).

$$\varepsilon = \frac{\sigma}{E} + \left(\frac{\sigma}{K}\right)^n \quad (5)$$

where *n* is the Ramberg–Osgood coefficient listed in Table 2, whilst *K* is the cyclic strain coefficient obtained from data regression of the coupon stress and associated plastic strain values. It is noted that the data points were taken as an average of the positive and negative point values from the hysteretic response for each tested coupon. The resulting envelope curves superimposed over the experimental data in Figure 9. The power function is seen to be effective in approximating the peaks of the cyclic stress–strain response for *K* coefficient value equal to 335.

4 Conclusions

This paper presents preliminary results of an experimental campaign which aims to investigate the nonlinear stress-strain behaviour of 6000 series aluminium alloys. Particularly, the experimentally obtained hysteretic behaviour of 6082-T6 aluminium alloy is presented and discussed herein. A total of 6 coupon tests were performed including 3 under monotonic tensile loading and 3 under cyclic loading up to 6.5% amplitude. The obtained results are reported and discussed, and the following conclusions are drawn:

- The monotonic stress–strain behaviour of the 6082-T6 aluminium alloy can be approximated accurately by the two-stage model proposed by Yun et. Al [10].
- The hysteretic curves obtained from the cyclic coupon tests are relatively plump denoting satisfactory hysteretic behaviour and adequate energy dissipation capacity of the examined aluminium alloy.
- At increased strain demands and by the end of the tests, the examined aluminium alloy exhibited hardening behaviour without material degradation.
- The Ramberg–Osgood model [20] can precisely describe the cyclic envelope curves of 6082-T6 aluminium alloy.

Overall, the results reported herein demonstrate the potential of 6082-T6 aluminium alloy for structural applications located in earthquake prone areas. However, further research is needed on additional 6,000 series aluminium alloys to extend the pool of performance data and obtain a better understanding about their hysteretic behaviour. Finally, a constitutive material model needs to be developed to simulate the hysteretic behaviour of 6,000 series aluminium alloys and thus being employed in advanced numerical modelling studies.

Acknowledgments

The authors are grateful to the technicians of the School of Engineering of University of Southampton for their valuable assistance during the preparation of specimens and the conduction of the experiments.

References

[1] https://wecount.ma/en/casablanca-finance-city-cfc [accessed on 10 April 2023]

[2] https://www.metalworkingworldmagazine.com/abu-dhabis-ferrari-world-is-the-largest-aluminium-roof-in-the-world/ [accessed on 10 April 2023]

[3] Nip, KH.; Gardner, L.; Davies, CM.; Elghazouli, AY. (2010) *Extremely low cycle fatigue tests on structural carbon steel and stainless steel*. *Journal of Constructional Steel Research*, 66 (1), pp. 96–110.

[4] Shi, YJ.; Wang, M.; Wang, YQ. (2011) *Experimental and constitutive model study of structural steel under cyclic loading*. *Journal of Constructional Steel Research*, 67(8), pp. 1185–97.

[5] Baehre, R. (1966) *Trycktastravorav elastoplastikt material-nagrafragestallningar (Comparison between structural behaviour of elastoplastic material). Tekn Arne Johnson Ingenjorsbyra*.

[6] De Matteis, G.; Brando, G.; Mazzolani, FM. (2012) *Pure aluminium: An innovative material for structural applications in seismic engineering. Construction and Building Materials*, 26(1), pp. 677–86.

[7] Guo, X.; Shen, Z.; Li, Y. (2007) *Stress-strain relationship and physical-mechanical properties of domestic structural aluminum alloy. Journal of Building Structures*, 6, pp. 110–7.

[8] Steinhardt, PJ.; Nelson, DR.; Ronchetti, M. (1983) *Bond-orientational order in liquids and glasses. Physical Review B*, 28, pp. 784–805.

[9] Wang, Y.; Fan, F.; Qian, H.; Zhai, X. (2013) *Experimental study on constitutive model of high-strength aluminum alloy 6082–T6. Journal of Building Structures*, 34(6), pp. 113–20.

[10] Yun, X.; Wang, Z.; Gardner, L. (2021) *Full-range stress–strain curves for aluminum alloys. Journal of Structural Engineering*, 1;147(6):04021060.

[11] Georgantzia, E.; Gkantou, M.; Kamaris, GS. (2021) *Aluminium alloys as structural material: A review of research. Engineering Structures, 227:* 111372.

[12] Hopperstad, OS.; Langseth, M.; Remseth, S. (1995) *Cyclic stress-strain behaviour of alloy AA6060, Part I: Uniaxial experiments and modelling. International Journal of Plasticity*, 11(6), pp. 725–39.

[13] Chaboche, JL. (1989) *Constitutive equations for cyclic plasticity. International Journal of Plasticity*, 5, pp. 247–302.

[14] Hopperstad, OS.; Langseth, M.; Remseth, S. (1995) *Cyclic stress-strain behaviour of alloy AA6060 T4, Part II: Biaxial experiments and modelling. International Journal of Plasticity*, 11(6), pp. 741–62.

[15] Dusicka, P.; Tinker, J. (2013) *Global restraint in ultra-lightweight buckling-restrained braces. Journal of Composites for Construction*, 17(1), pp. 139–50.

[16] Guo, X.; Wang, L.; Shen, Z.; Zou, J.; Liu L. (2018) *Constitutive model of structural aluminum alloy under cyclic loading. Construction and Building Materials*, 180, pp. 643–54

[17] *European Committee for Standardization (CEN). Metallic Materials – Tensile Testing – Part 1: Method*

Of Test At Room Temperature. Brussels, 2009.

[18] *ASTM E606-04: Standard Practice for Strain-Controlled Fatigue Testing. Subcommittee E08.05 on Cyclic Deformation and Fatigue Crack Formation*, 2017.

[19] Kashani, MM.; Crewe, A.J.; Alexander, N.A. (2013) *Nonlinear cyclic response of corrosion-damaged reinforcing bars with the effect of buckling*. *Construction and Building Materials*, 41, pp.388–400.

[20] Ramberg, W.; Osgood, WR. (1943) *Description of stress-strain curves by three parameters. Vol. Technical.* Washington, D.C.: National Advisory Committe for Aeronautics.

[21] Hill, HN.; Clark, JW.; Brungraber, RJ. (1960) *Design of welded aluminum structures. Journal of the Structural Divivsion*, *ASCE*, 86(6), pp. 101–24.